Article

Nonvesicular Inhibitory Neurotransmission via Reversal of the GABA Transporter GAT-1

Yuanming Wu,[1] Wengang Wang,[1] Ana Díez-Sampedro,[1,4] and George B. Richerson[1,2,3,*]
[1]Department of Neurology
[2]Department of Cellular and Molecular Physiology
Yale University School of Medicine, New Haven, CT 06510, USA
[3]Neurology Service, Veteran's Affairs Medical Center, West Haven, CT 06516, USA
[4]Present address: Department of Physiology and Biophysics, Miller School of Medicine, University of Miami, Miami, FL 33136, USA.
*Correspondence: george.richerson@yale.edu

SUMMARY

GABA transporters play an important but poorly understood role in neuronal inhibition. They can reverse, but this is widely thought to occur only under pathological conditions. Here we use a heterologous expression system to show that the reversal potential of GAT-1 under physiologically relevant conditions is near the normal resting potential of neurons and that reversal can occur rapidly enough to release GABA during simulated action potentials. We then use paired recordings from cultured hippocampal neurons and show that GABAergic transmission is not prevented by four methods widely used to block vesicular release. This nonvesicular neurotransmission was potently blocked by GAT-1 antagonists and was enhanced by agents that increase cytosolic [GABA] or [Na$^+$] (which would increase GAT-1 reversal). We conclude that GAT-1 regulates tonic inhibition by clamping ambient [GABA] at a level high enough to activate high-affinity GABA$_A$ receptors and that transporter-mediated GABA release can contribute to phasic inhibition.

INTRODUCTION

Many synaptic physiologists view GABA transporters as always operating in uptake mode, continuously working at their maximum rate of uptake, and being capable of nearly completely eliminating all GABA from the extracellular space. However, this view is not consistent with the thermodynamics of transporters. Instead, it is well known that transporters can reverse (Attwell et al., 1993; Cammack et al., 1994; Levi and Raiteri, 1993; Lu and Hilgemann, 1999; O'Malley et al., 1992; Pin and Bockaert, 1989; Schwartz, 1987), there is indirect evidence that they are near equilibrium (and thus relatively inactive) under resting conditions (Richerson and Wu, 2003), and

there is a theoretical limit to how much they can reduce ambient [GABA] (Attwell et al., 1993; Cavelier et al., 2005; Richerson and Wu, 2003).

It is widely believed that reversal of GABA transporters is uncommon except under pathological conditions. However, there is theoretical and indirect experimental evidence that the membrane potential at which GABA transporters reverse is close to the normal resting potential of neurons. For example, GAT-1 (the neuronal isoform of the GABA transporter) can be induced to reverse in hippocampal cultures by a small depolarization of membrane potential caused by 6 mM K$^+$ (Wu et al., 2001) or by an increase in cytosolic [GABA] caused by the anticonvulsant vigabatrin (Richerson and Wu, 2003; Wu et al., 2001, 2003). The reversal potential of an electrogenic transporter can be calculated if its stoichiometry is known (Aronson et al., 2003; Richerson and Wu, 2003). For GAT-1, which is believed to undergo coupled translocation of Na$^+$, Cl$^-$, and GABA in a ratio of 2:1:1 (Kanner and Schuldiner, 1987; Lu and Hilgemann, 1999), the theoretical reversal potential is close to the normal resting potential of neurons when ambient [GABA] is 0.1–0.4 μM (Attwell et al., 1993; Richerson and Wu, 2003). If true, this is surprising because it suggests that GAT-1 would stop taking up GABA even though ambient [GABA] is high enough to activate high-affinity GABA$_A$ receptors (Saxena and Macdonald, 1996), and thus GAT-1 would not be capable of lowering ambient [GABA] enough to eliminate tonic inhibition of neurons expressing these receptors. Determining whether these calculations of reversal potential are accurate is important because it allows predictions about the behavior of GAT-1 and its role in synaptic and extrasynaptic inhibition.

Several groups have directly measured transporter currents to determine whether GAT-1 operates as predicted by classical models (Cammack et al., 1994; Krause and Schwarz, 2005; Lu and Hilgemann, 1999; Mager et al., 1993). Using this approach, it has been verified that the magnitude of GAT-1 transporter currents is altered in response to changes in sodium, chloride, and GABA gradients as would be predicted if GABA translocation is coupled to 2 Na$^+$ and 1 Cl$^-$ (Lu and Hilgemann, 1999). However, the methods used to make these measurements were relatively insensitive, making it necessary to

use nonphysiological concentrations of substrate (e.g., 120 mM intracellular [Na$^+$], 60 mM intracellular [Cl$^-$], and/or 2 mM extracellular [GABA]) to increase the size of transporter currents. It has not yet been possible to measure the reversal potential of GAT-1 using this approach under physiological conditions. Recordings of transporter current also do not directly measure GABA flux, and there can be Na$^+$ flux in the absence of GABA flux (i.e., uncoupled current) (Cammack et al., 1994; Krause and Schwarz, 2005). GABA flux has been measured directly using biochemical and radioactive assays (Belhage et al., 1993; Pin and Bockaert, 1989; Schwartz, 1982; Turner and Goldin, 1989), but these assays of GABA release do not allow reversal potential to be determined. A variety of indirect methods have also been used to determine how easily GAT-1 will reverse (Wu et al., 2001, 2003, 2006), but these lack the experimental control needed to quantify the reversal potential.

Here we describe an assay to measure the reversal potential of a GABA transporter. One set of CHO cells was transfected with GAT-1 ("GAT-1 cells"). Another set of CHO cells was transfected with high-affinity GABA$_A$ receptors ("sniffer cells") and was used to detect GABA release from the GAT-1 cells. Using this approach, we demonstrate that GAT-1 behaves as predicted by classical models, reverses under physiological conditions, and is more dynamic than commonly believed. We then used paired recordings from hippocampal neurons in culture to demonstrate that these results are relevant to normal GAT-1 function. In this preparation, we found that IPSCs still occur after blocking vesicular neurotransmission, and this is due to GAT-1 reversal. Taken together, these results indicate that GAT-1 plays an important role in regulation of tonic inhibition and identify a primitive form of neurotransmission that can maintain phasic inhibition when there is failure of vesicular neurotransmitter release.

RESULTS

Detection of GAT-1 Reversal with a Sniffer Cell Assay

GABA$_A$ receptors that include the δ subunit are highly sensitive to low levels of GABA (EC$_{50}$ 0.2–0.4 μM) and have relatively little desensitization (Bianchi et al., 2002; Saxena and Macdonald, 1996). The δ subunit is coexpressed with α6 subunits in cerebellar neurons, where it plays an important role in mediating tonic inhibition (Brickley et al., 2001). We took advantage of the high affinity of δ subunit-containing GABA$_A$ receptors to measure transporter-mediated GABA release using a functional assay. Patch-clamp recordings were made in whole-cell voltage-clamp mode (holding potential = −60 mV) from CHO cells transfected with the α6, β3, and δ subunits of the GABA$_A$ receptor. In successfully transfected (green fluorescent protein [GFP]-expressing) sniffer cells, bath application of GABA at 0.1 μM induced a current (−871 ± 82 pA; n = 5; E$_{Cl}$ = 0 mV) (see Figure S1A available online) that was blocked by bicuculline (50 μM) (−24 ± 12 pA; n = 5). This current

was not induced in CHO cells that underwent the transfection procedure but did not express GFP (−3 ± 5 pA; n = 5).

Patch-clamp recordings were also made from a separate set of CHO cells transfected with GAT-1 cDNA. These GAT-1 cells were lifted off their coverslip and positioned so they were touching the surface of sniffer cells (Figure 1A). For this first set of experiments, the electrode (intracellular) solution used for recording from the GAT-1 cell contained 30 mM Na$^+$, 30 mM Cl$^-$, and 5 mM GABA, concentrations that were chosen to be higher than physiological to increase the chance of reversal so that we could determine whether our approach was feasible. An example of a voltage-clamp recording from a sniffer cell under these conditions is shown in Figure S1B. An inward current was induced in the sniffer cell when the GAT-1 cell was voltage clamped at a potential of −60 mV, and this current increased when the membrane potential of the GAT-1 cell was increased. The response of the sniffer cell was dependent upon the proximity of the GAT-1 cell, because the current induced in the sniffer cell decreased when the two cells were moved apart from each other, and increased when they were brought back together (n = 6).

Progressively more depolarizing voltages applied to the GAT-1 cell (−80 mV to +40 mV) led to progressively larger inward current in the sniffer cell (Figure 1B; −1002 ± 174 pA at +40 mV; n = 11). The response was blocked by bicuculline (50 μM; 8% ± 4% of control; n = 9; p < 0.001), indicating that it was due to activation of GABA$_A$ receptors. CHO cells do not contain synaptic vesicles or the vesicular GABA transporter vGAT, so the response was not due to vesicular GABA release. The response was also not calcium dependent, since the sniffer cell response in Ringer with 0 mM Ca^{2+} was 91% ± 11% of that in normal Ringer (n = 9; p > 0.05). Instead, the inward current was blocked by the GAT-1 antagonist SKF-89976a (40 μM; 4% ± 1% of control; n = 8; p < 0.001). There was no response when CHO cells were used that underwent the transfection procedure for GAT-1 but did not express GFP (n = 5). We conclude that the response in the sniffer cell was due to activation of GABA$_A$ receptors by GABA released from the GAT-1 cell via transporter reversal.

Previous experiments have measured reversal potentials by directly recording transporter currents in cells transfected with GAT-1 (Cammack et al., 1994; Lu and Hilgemann, 1999). We found that approach to be much less sensitive than measuring GABA release using the sniffer cell assay. Whole-cell patch-clamp recordings were made from GAT-1 cells using an electrode solution containing 15 mM Na$^+$, 10 mM Cl$^-$, and 2 mM GABA (Figure 1C)—intracellular concentrations that have been reported by others to occur in some adult mammalian neurons (Otsuka et al., 1971; Rose, 2002; Rose and Ransom, 1997; Schwartz, 1987; Zhu et al., 2005). As GAT-1 cells were depolarized using a voltage-ramp protocol (Figure 1D, top panel), a large inward current developed in neighboring sniffer cells (peak current 336 ± 46 pA, n = 8; Figure 1D, middle panel, black trace). At the same
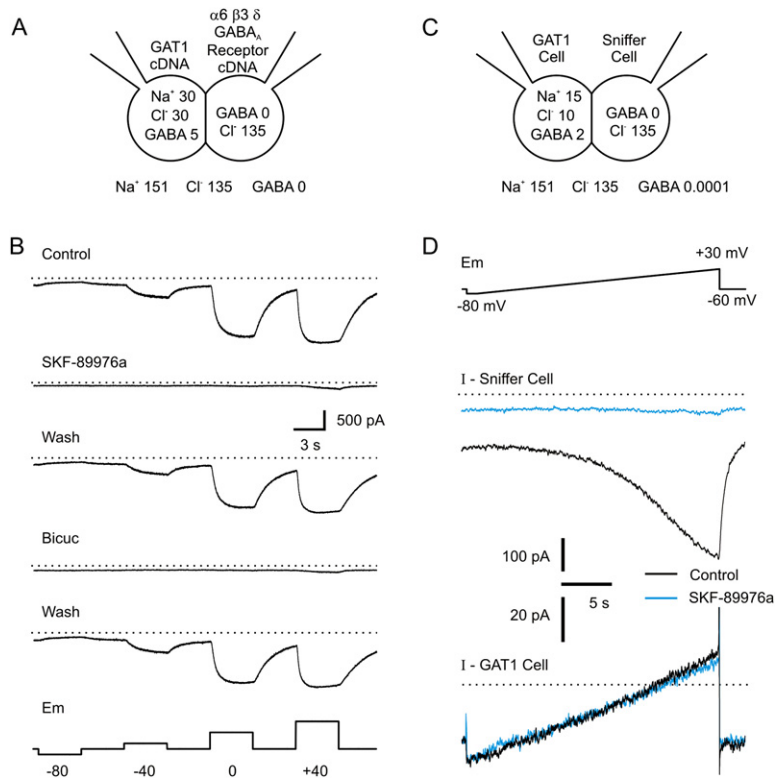
Figure 1. Assay for Detecting GABA Release via GAT-1 Reversal

(A) Patch-clamp recordings were made from two CHO cells, one transfected with the $\alpha 6$, $\beta 3$, and δ subunits of the $GABA_A$ receptor (sniffer cell) and the other with GAT-1 (GAT-1 cell). The concentrations of Na^+, Cl^-, and GABA were systematically controlled in the inside and on the outside of the GAT-1 cell.

(B) Using the concentrations of substrate shown in (A), hyperpolarization from −60 mV to −80 mV led to a decrease in inward current in the sniffer cell, whereas depolarization to −40, 0, and +40 mV led to a progressively larger inward current. The current was due to GABA release from GAT-1 reversal, because it was blocked by bicuculline (50 μM) and SKF-89976a (40 μM).

(C) Concentrations of Na^+, Cl^-, and GABA used for experiments in (D). These concentrations of substrate are within a range reported to occur in some CNS neurons (see text).

(D) The CHO cell assay detected reversal of GAT-1 more sensitively than when transporter currents were measured directly. (Top panel) GAT-1 cells were depolarized with a ramp protocol. (Middle panel) GABA release was detected as a large inward current (black trace) induced in the sniffer cell in response to ramp depolarization of the GAT-1 cell. This current was blocked by SKF-89976a (40 μM; blue trace). (Bottom panel) There was not any measurable transporter current in the GAT-1 cell, which would have been detected as a change in whole-cell current in the GAT-1 cell in response to SKF-89976a (black trace, control; blue trace, SKF-89976a). Dotted line in middle panel is −400 pA and in bottom panel is 0 pA.

time, there was a leak current measured in GAT-1 cells during the ramp protocol (Figure 1D, bottom panel, black trace). SKF-89976a (40 μM) completely blocked the inward current in sniffer cells (5% ± 4% of control; n = 8; p < 0.001) (Figure 1D, middle panel, blue trace). However, there was not a consistent effect of SKF-89976a on the leak current in the GAT-1 cells (change in slope conductance of GAT-1 cells induced by SKF-89976a = −0.09 ± 0.10 nS; Figure 1D, bottom panel, blue trace; n = 6; p > 0.05). This indicates that the current mediated by GAT-1 is too small to be detected by directly recording from the GAT-1 cell (consistent with previous reports, as discussed above). However, GAT-1 reversal could be monitored indirectly by detecting GABA efflux using our sniffer cell assay.

The Reversal Potential for GAT-1 Is Near Resting Potential under Physiological Conditions

We next determined the minimum voltage at which GAT-1 reversal could be detected under the physiologically relevant conditions used in the previous experiment. Whole-cell voltage-clamp recordings were made from GAT-1 cells using the electrode solution with 15 mM Na^+, 10 mM Cl^-, and 2 mM GABA and a bath solution with

151 mM Na^+, 135 mM Cl^-, and 0.1 μM GABA. A slow ramp depolarization was repeated three to six times, and the mean sniffer cell current was plotted (Figure 2A, black trace). A moving average was then calculated from the mean current (Figure 2A, green trace). The voltage in the GAT-1 cell at which an increase in inward current was first detected in the sniffer cell (i.e., ambient [GABA] first began to rise) was estimated to be the reversal potential for GAT-1. For the recording in Figure 2A, the reversal potential measured using this method was −69.5 mV. For recordings from 12 cell pairs, the mean reversal potential under these conditions was −67.1 ± 6.47 mV, which was close to the theoretical reversal potential of −68.2 mV (see Experimental Procedures). Thus, as predicted, the reversal potential of GAT-1 under these physiologically relevant conditions is near the normal membrane potential of many neurons. This may be surprising, because it indicates that GAT-1 would be at equilibrium under resting conditions, and there would be no GABA uptake, even when ambient [GABA] is near the normal level of around 0.1 μM (see Discussion). As shown in Figure S1A and previously (Bianchi et al., 2002; Saxena and Macdonald, 1996), this [GABA] is high enough to activate high-affinity $GABA_A$ receptors.
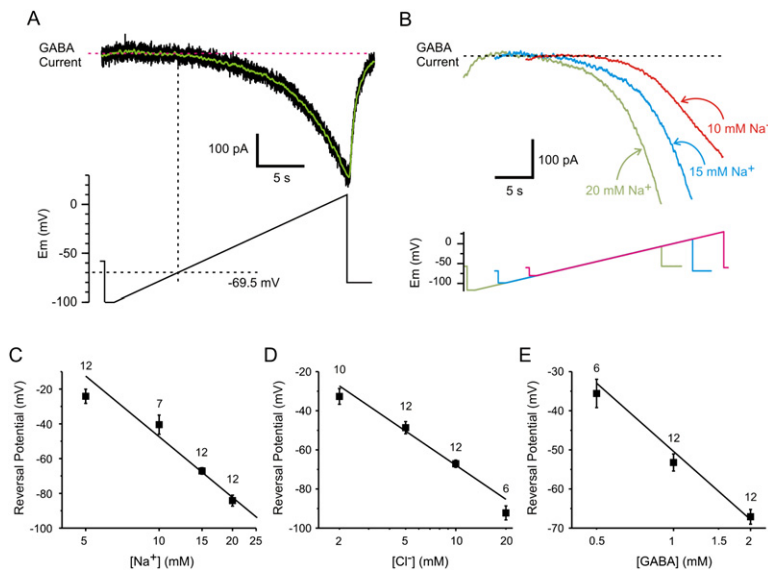
Figure 2. The Reversal Potential of GAT-1 Is Near Resting Potential under Physiological Conditions and Shifts as Predicted for a Stoichiometry of 2 Na$^+$:1 Cl$^-$:1 GABA

(A) Method used to measure the reversal potential of GAT-1. Shown is the current induced in a sniffer cell (top panel, black trace; average of six trials) in response to ramp depolarization (bottom panel) of a GAT-1 cell. A moving average (green trace) was calculated from the mean current. A horizontal line was drawn through the flat portion of the trace, and then a vertical line was drawn at the time that the inward current first began to increase. The intersection of the vertical line with the voltage-clamp command was used to determine the reversal potential, which was −69.5 mV in this example.

(B) The reversal potential shifted to hyperpolarized levels when cytosolic [Na$^+$] increased. Shown is the current induced in sniffer cells in response to ramp depolarization of three different GAT-1 cells in which the cytosolic [Na$^+$] ranged from 10 mM to 20 mM.

(C) Effect of cytosolic [Na$^+$] on reversal potential.
(D) Effect of cytosolic [Cl$^-$] on reversal potential.
(E) Effect of cytosolic [GABA] on reversal potential.
For (C)–(E) the squares are the mean (±SEM) of the measured reversal potential, the numbers above each square are the number of cells recorded, and the solid line is the theoretical reversal potential.

Thus, GAT-1 would not normally be able to eliminate tonic inhibition even in the absence of synaptic GABA release.

GABA Transport Remains Coupled to 2 Na$^+$ and 1 Cl$^-$

The uncoupled mode described for GAT-1 involves sodium flux in the absence of GABA transport (Krause and Schwarz, 2005). However, it is not known whether GAT-1 can operate in an uncoupled mode in which GABA flux occurs in the absence of Na$^+$ and Cl$^-$ transport, and there have been no methods previously available to determine whether this is true under near-physiological conditions. If GABA transport is always coupled to Na$^+$ and Cl$^-$, then the equations for the driving force on the transporter should accurately predict changes in the reversal potential of GAT-1 in response to changes in the transmembrane gradients for Na$^+$, Cl$^-$, and GABA (Aronson et al., 2003; Attwell et al., 1993; Richerson and Wu, 2003).

We measured the reversal potential of GAT-1 while systematically varying [Na$^+$], [Cl$^-$], or [GABA] in the whole-cell patch-clamp electrode solutions used to record from different cells. The reversal potential of GAT-1 shifted progressively to more negative values as intracellular [Na$^+$] increased (Figure 2B). The experimentally measured reversal potential of GAT-1 shifted from −24.2 mV to −84.2 mV as intracellular [Na$^+$] was changed from 5 mM to 20 mM (Figure 2C). The change in reversal potential was measured to be −99.7 mV per 10-fold change in [Na$^+$]$_i$ (calculated as the slope of the linear regression), compared to the predicted value of −117.1 mV. The differ-

ence was due to a small divergence from the theoretical prediction at 5 mM, which was likely due to instability of the recording at higher membrane potentials.

Similar experiments were performed using different concentrations of chloride in the pipette solution. There was a shift in reversal potential of GAT-1 from −32.7 mV to −92.2 mV as intracellular [Cl$^-$] was changed from 2 mM to 20 mM (Figure 2D). Note that the reversal potential is more steeply dependent on the sodium gradient than the chloride gradient, since there are twice as many Na$^+$ ions transported per translocation cycle. Theoretical calculations predict that there is a −58.5 mV shift in reversal potential with a 10-fold change in the chloride gradient, which was close to the experimentally measured value of −58.7 mV.

Even though GABA carries no net charge, a change in the GABA concentration gradient would be expected to shift the reversal potential of GAT-1 if GABA transport is obligately coupled to 2 Na$^+$ and 1 Cl$^-$. As predicted, a change in intracellular [GABA] from 0.5 mM to 2 mM led to a shift in the experimentally measured reversal potential of GAT-1 from −35.6 mV to −67.1 mV (Figure 2E). The shift in reversal potential was found to be −50.7 mV per 10-fold change in the GABA gradient, which was close to the theoretical value of −58.5 mV.

Our sniffer cell assay only allowed us to measure GABA efflux, and not influx, requiring that we extrapolate our measurements to estimate the reversal potential. This may have led to an error, but the close correlation with the theoretical reversal potential suggests that the error
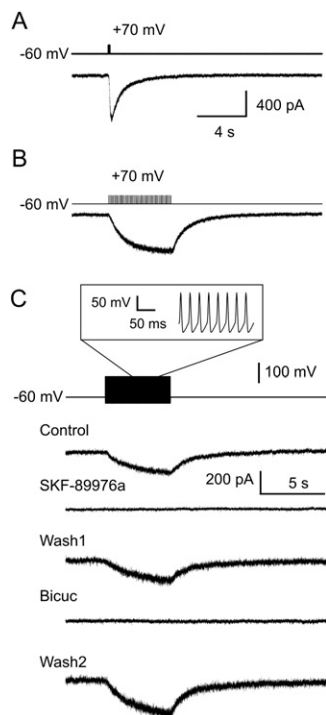
Figure 3. GAT-1 Reverses during Simulated Action Potentials

(A) A single depolarizing 100 ms square wave pulse from −60 mV to +70 mV induced a large response in a sniffer cell.

(B) Current was also induced in a sniffer cell by a train of 10 ms depolarizing pulses from −60 mV to +70 mV (frequency 10 Hz; train duration 5 s).

(C) Simulated action potentials induced a response in a sniffer cell. The command voltage for the GAT-1 cell was a waveform (inset) that simulated a train of action potentials at a rate of 40 Hz. The resting potential was −60 mV, peak voltage was +40 mV, and action potential duration was 6 ms. The response in the sniffer cell was due to GABA release via GAT-1 reversal, because it was blocked by both SKF-89976a (40 μM) and bicuculline (50 μM).

was small, probably because the GABA receptor subunits we used were able to detect GABA release from the GAT-1 cell soon after it began to occur. If there was an error, our approach provides an upper limit for the reversal potential, making our finding of a low reversal potential even more significant.

We cannot rule out the possibility that an uncoupled Na^+ current (Krause and Schwarz, 2005) occurred in our experiments, since our assay would not detect it. However, our results do indicate that GAT-1 does not allow spontaneous GABA efflux via a channel-like mode, as occurs with the dopamine transporter in response to amphetamine (Kahlig et al., 2005), and when GABA flux does occur it remains coupled to 2 Na^+ and 1 Cl^- when the substrates are near physiological concentrations.

GAT-1 Operates Rapidly Enough to Reverse during an Action Potential

We next examined how rapidly GAT-1 reverses. Recordings were made from CHO cells in voltage-clamp mode

at a holding potential of −60 mV using an electrode solution containing 30 mM Na^+, 30 mM Cl^-, and 5 mM GABA. The bath solution contained 151 mM Na^+, 135 mM Cl^-, and no GABA. A large inward current was induced in sniffer cells in response to a 100 ms depolarizing pulse to +70 mV in GAT-1 cells (−379 ± 71 pA; Figure 3A; n = 5). A train of 10 ms pulses to +70 mV at 10 Hz also induced an inward current, this time with a more gradual onset (−207 ± 48 pA; Figure 3B; n = 9).

Based on the data presented above, we considered whether GAT-1 might reverse rapidly enough to release GABA during an action potential. To test this hypothesis, we simulated action potentials in CHO cells (which do not generate action potentials on their own) by varying the voltage command supplied to the amplifier using a waveform that replicated action potentials previously recorded from cultured rat neurons. In response to a train of 200 simulated action potentials at a rate of 40 Hz, an inward current was generated in sniffer cells (−76 ± 13 pA; Figure 3C; n = 12). This current was due to GABA release via GAT-1 reversal since it was blocked by SKF-89976a (40 μM; −1% ± 2% of control; n = 10; p < 0.001) and bicuculline (50 μM; 4% ± 3% of control; n = 8; p < 0.005) (Figure 3C). Although the substrate gradients used were not as close to physiological as in Figure 2A, a change in the concentration gradients for substrate would not alter the rapidity with which GAT-1 would reverse. Instead, it would only alter the reversal potential, which we have already shown is close to normal resting potential under physiological conditions. Thus, these data indicate that GAT-1 should operate rapidly enough to reverse and release GABA during action potentials in neurons.

GAT-1 Can Mediate GABAergic Transmission between Hippocampal Neurons

To determine whether GABA release due to GAT-1 reversal can occur during action potentials in neurons, we performed patch-clamp recordings from pairs of rat hippocampal neurons grown in primary dissociated cell culture. Unless otherwise noted, cultures were pretreated with the GABA transaminase inhibitor vigabatrin to enhance transporter-mediated GABA release (Richerson and Wu, 2003; Wu et al., 2001, 2003). In Ringer containing 2 mM Ca^{2+}, electrical stimulation of presynaptic GABAergic neurons led to an inhibitory postsynaptic current (IPSC) that was blocked by bicuculline (50 μM; n = 8). When $[Ca^{2+}]_o$ was decreased to 0.2 mM and $[Mg^{2+}]_o$ was increased to 10 mM, IPSCs were blocked in response to single presynaptic action potentials (n = 12). However, IPSCs could still be elicited in response to high-frequency stimulation of 76% of GABAergic synapses (n = 34 of 45; 50 Hz stimulation for 9 s; Figure 4A). These IPSCs were blocked by the GABA$_A$ receptor antagonists gabazine (Figure 4A; 200–400 nM; 13% ± 4% of control; n = 14; p < 0.001) and bicuculline (Figure S2A; 50 μM; −2% ± 1% of control; n = 8; p < 0.005). Both antagonists also induced a shift in baseline holding current (bicuculline: −292 ± 59 pA; gabazine: −81 ± 22 pA), consistent with blockade
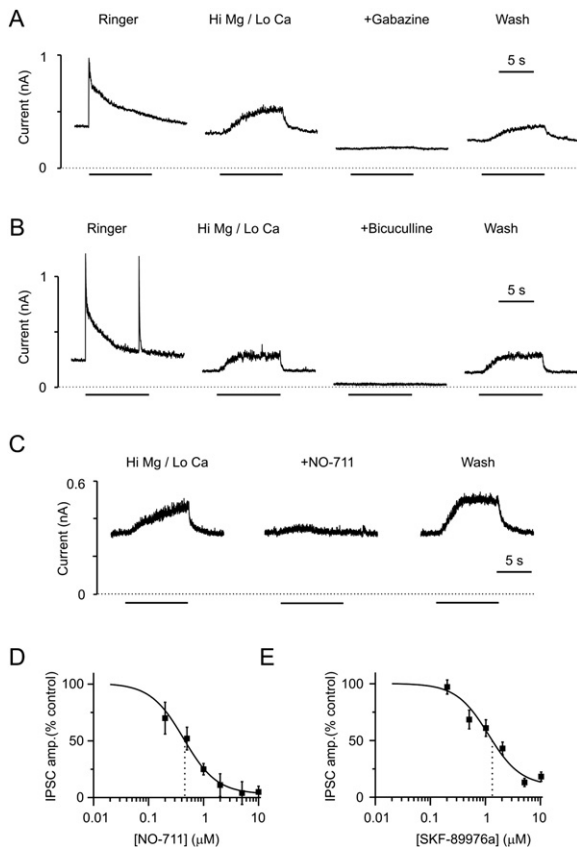
Figure 4. GABAergic Synaptic Transmission Occurs between Hippocampal Neurons in High Mg^{2+} (10 mM)/Low Ca^{2+} (0.2 mM) Ringer and Is Blocked by GAT-1 Antagonists

(A) Dual patch-clamp recordings from a pair of rat hippocampal neurons in culture after pretreatment with vigabatrin (100 μM; 128 hr). Shown are IPSCs in response to high-frequency presynaptic stimulation (50 Hz for 9 s). The first trace was recorded in Ringer with 2 mM Ca^{2+}. The next three traces were made in high Mg^{2+}/low Ca^{2+} Ringer. The IPSCs were blocked by gabazine (400 nM).

(B) IPSCs could also be obtained in high Mg^{2+}/low Ca^{2+} solution from neurons that had not been treated with vigabatrin.

(C) IPSCs in high Mg^{2+}/low Ca^{2+} Ringer were blocked by NO-711 (10 μM). Bars in (A)–(C) indicate time of presynaptic stimulation.

(D) Concentration/response curve for NO-711. Each data point represents seven to nine different neuron pairs in high Mg^{2+}/low Ca^{2+} Ringer. Solid line is a logistic fit (Microcal Origin). IC$_{50}$ was 0.43 μM.

(E) Concentration/response curve for SFK-89976a. Each data point represents 8 to 13 different neuron pairs in high Mg^{2+}/low Ca^{2+} Ringer. IC$_{50}$ was 1.3 μM.

For (D) and (E), error bars are SEM.

of the tonic GABAergic inhibition that is induced by vigabatrin (Overstreet and Westbrook, 2001; Wu et al., 2001, 2003). A postsynaptic response could also be elicited in high Mg^{2+}/low Ca^{2+} solution without pretreatment with vigabatrin (Figure 4B), although not as frequently (48% of GABAergic synapses; n = 15 of 31).

An increase in the ratio of Mg^{2+} to Ca^{2+} to 20:1 is widely used to block vesicular release. Therefore, maintenance of synaptic transmission with a Mg^{2+} to Ca^{2+} ratio of 50:1

is consistent with the hypothesis that the IPSCs that occurred were due to reversal of GABA transporters. In support of this hypothesis, GABAergic IPSCs in high Mg^{2+}/low Ca^{2+} solution were blocked by two GAT-1-specific antagonists, NO-711 (5–50 μM; Figure 4C; n = 27) and SKF-89976a (5–40 μM; Figure S2B; n = 56). The response was blocked in a concentration-dependent manner (Figures 4D and 4E), with an IC$_{50}$ for both drugs (SKF-89976a, 1.3 μM; NO-711, 0.43 μM) near that reported previously for blockade of GABA uptake (SKF-89976a, 0.2 μM [Yunger et al., 1984]; NO-711, 0.38 μM [Borden, 1996]). During whole-cell recordings, GAT-1 blockade induces a shift in holding current that can either be inward or outward, depending upon the recording conditions (Richerson and Wu, 2003; Wu et al., 2003). The direction and amplitude of this shift in tonic current was unrelated to the ability of NO-711 and SKF-89976a to block IPSCs in high Mg^{2+}/low Ca^{2+} solution.

It is hard to explain why specific GAT-1 antagonists would block IPSCs in high Mg^{2+}/low Ca^{2+} solution other than by blocking GAT-1 reversal. It is unlikely that there was residual vesicular GABA release that was blocked by SKF-89976a and NO-711, because we found that IPSCs induced in normal calcium Ringer were not affected by either agent (peak amplitudes: 89% ± 14% of control in 50 μM NO-711, n = 8, p > 0.05; 98% ± 7% of control in 40 μM SKF-89976a, n = 9, p > 0.05). Other investigators have also seen either no effect or an increase in the amplitude of vesicular IPSCs in response to GABA transporter blockers, including GAT-1-selective antagonists (Dingledine and Korn, 1985; Isaacson et al., 1993; Nusser and Mody, 2002; Overstreet and Westbrook, 2003; Roepstorff and Lambert, 1992; Thompson and Gahwiler, 1992).

To rule out the possibility that the IPSCs we observed in high Mg^{2+}/low Ca^{2+} solution were due to residual calcium influx causing vesicular GABA release, we used pretreatment with tetanus toxin as an alternative method to block vesicular GABA release. Cultures were pretreated with 10 μg/ml of tetanus toxin for >24 hr (27.5 ± 0.5 hr), a concentration one to ten times greater than that previously shown to block GABAergic vesicular release (Albus and Habermann, 1983; Pearce et al., 1983; Pin and Bockaert, 1989). This also did not completely block IPSCs, which could still be elicited in response to high-frequency stimulation (Figure 5A; n = 10). The response after tetanus toxin treatment was blocked by bicuculline (Figure 5A; 50 μM; 1% ± 1% of control; n = 4; p < 0.01) and by SKF-89976a (Figure 5A; 40 μM; 8% ± 8% of control; n = 5; p > 0.005). IPSCs were also seen in 11 neuron pairs pretreated with 5 μg/ml tetanus toxin (28 ± 0.5 hr), and these were also blocked by bicuculline (50 μM; n = 3) and SKF-89976a (40 μM; n = 6).

Pin and Bockaert (1989) previously reported that GABA release induced from cultured striatal neurons (measured using HPLC) is not prevented by removal of extracellular calcium, treatment with tetanus toxin, or both. Similar to those results, we found that the combination of tetanus toxin and high Mg^{2+}/low Ca^{2+} solution did not block
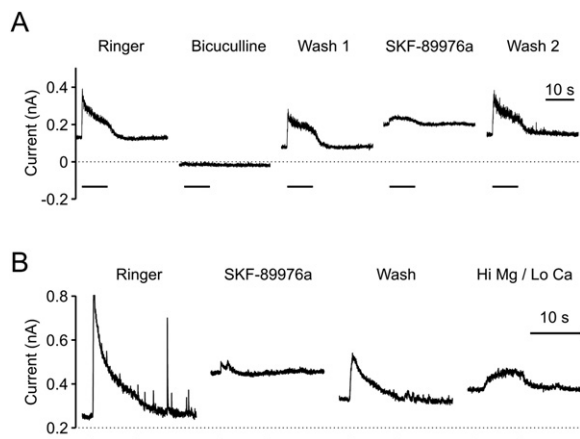
Figure 5. GABAergic Synaptic Transmission Also Occurred after Treatment with Tetanus Toxin, and Was Blocked by GAT-1 Antagonists

(A) IPSC in a neuron pretreated with 10 μg/ml tetanus toxin (27 hr) and vigabatrin (100 μM; 100 hr). The IPSC was blocked by bicuculline (50 μM) and by SKF-89976a (40 μM). Recording was made in Ringer with 2 mM Ca^{2+}.

(B) IPSC in a neuron pretreated with 5 μg/ml tetanus toxin (30 hr) and vigabatrin (100 μM; 124 hr). The IPSC was blocked by SKF-89976a (40 μM) while recording in Ringer with 2 mM Ca^{2+}. IPSCs could also be elicited from this neuron in high Mg^{2+}/low Ca^{2+} Ringer (last trace). Bars, presynaptic stimulation.

IPSCs. In six neurons pretreated with tetanus toxin (5–10 μg/ml; 28 ± 0.8 hr) in which IPSCs could be induced in normal calcium solution, IPSCs could also be induced in high Mg^{2+}/low Ca^{2+} solution (Figure 5B). The waveform of IPSCs in tetanus toxin-treated neurons was different in Ringer with calcium than in high Mg^{2+}/low Ca^{2+} solution, with the former having a more rapid rise and a higher peak response, but followed by a decay to a similar steady-state amplitude as IPSCs in high Mg^{2+}/low Ca^{2+} solution (Figure 5B; steady-state response in 2 mM Ca^{2+} = 73 ± 23 pA; in 0.2 mM Ca^{2+} = 64 ± 9 pA; n = 6, p > 0.05).

Concanamycin A inhibits the vesicular H^+-ATPase and causes collapse of the proton gradient needed to load GABA into synaptic vesicles (Rossi et al., 2003). This agent is commonly used to block synaptic transmission. After pretreatment of hippocampal cultures with concanamycin A (0.5 μM; 2 hr), vesicular GABA release could no longer be induced by α-latrotoxin (Sudhof, 2001) (n = 9; Figures 6A and 6B), indicating that synaptic vesicles were effectively depleted of GABA. However, IPSCs could still be obtained by high-frequency stimulation of presynaptic neurons (n = 54). These IPSCs were mediated by reversal of GABA transporters, because they were blocked by NO-711 (10 μM; 12% ± 2% of control; n = 27/29; p < 0.001) (Figure 6C). After concanamycin A, IPSCs also occurred in neurons when recordings were made in high Mg^{2+}/low Ca^{2+} solution (n = 10) (Figure 6D). As was true after tetanus toxin treatment, high Mg^{2+}/low Ca^{2+} solution changed the waveform of IPSCs after concanamycin A treatment.
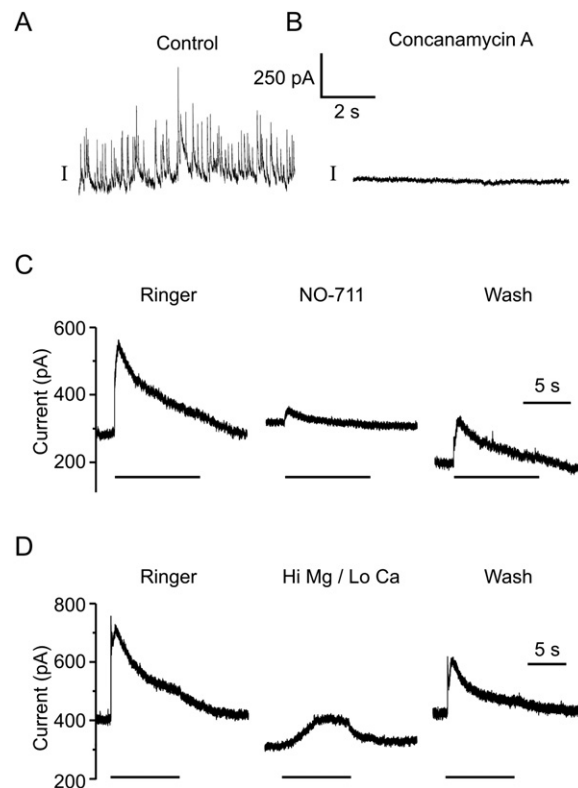

Figure 6. GABAergic Synaptic Transmission Occurred after Treatment with Concanamycin A, and Was Also Blocked by GAT-1 Antagonists

(A) α-latrotoxin (0.6 nM) caused a large amount of vesicular GABA release in control neurons.

(B) α-latrotoxin did not induce any vesicular release in neurons pretreated with concanamycin A (0.5 μM for 2 hr).

(C) IPSCs could still be induced in this neuron after pretreatment with concanamycin A. The response was decreased by NO-711 (10 μM).

(D) IPSCs could also be elicited in high Mg^{2+}/low Ca^{2+} Ringer after pretreatment with concanamycin A. Bars, presynaptic stimulation.

If the IPSCs described above are due to GAT-1 reversal, then they should be enhanced by an increase in the outward driving force on the GABA transporter, such as occurs with an increase in cytosolic $[Na^+]$ or [GABA] (Richerson and Wu, 2003; Wu et al., 2006). Consistent with this prediction, IPSCs were larger after treatment with vigabatrin, which increases cytosolic [GABA] and augments transporter-mediated GABA release (Wu et al., 2001, 2003). After treatment with vigabatrin (100 μM; 85 ± 6 hr), the amplitude of IPSCs was increased in high Mg^{2+}/low Ca^{2+} solution (589 ± 139 pC; n = 30) compared to untreated neurons (292 ± 69 pC; n = 33; p < 0.05). The enhancement by vigabatrin was unlikely to be due to enhancement of incompletely blocked vesicular neurotransmission, since vigabatrin does not increase vesicular GABA release (Overstreet and Westbrook, 2001; Wu et al., 2003).

The magnitude of IPSCs in high Mg^{2+}/low Ca^{2+} solution increased with presynaptic firing rate. At firing rates less

than 20 Hz, IPSCs could not be elicited from GABAergic synapses (n = 12). There was a small response at 20 Hz (77 ± 37 pC), and this increased further at 50 Hz (720 ± 101 pC). Although there are several possible explanations for this, it is consistent with an increase in driving force for GABA transporter reversal, since intracellular [Na$^+$] and mean membrane potential would both increase in presynaptic terminals with increasing firing rate.

Nonvesicular GABAergic Neurotransmission Can Occur in the Absence of Extracellular Ca^{2+}

The data described above from neurons support the conclusion that GAT-1 will reverse during action potentials. However, in contrast to these findings we observed that IPSCs only rarely occurred in Ringer with 0 mM Ca^{2+} with or without EGTA (n = 1 of >25 attempts). This was not because GAT-1 is directly dependent on Ca^{2+} (see above). Furthermore, IPSCs were blocked when cadmium (0.2–1 μM) was added to high Mg^{2+}/low Ca^{2+} solution (n = 9), as well as in high Mg^{2+}/low Ca^{2+} solution with a combination of ω-conotoxin MVIIA (1 μM) and ω-agatoxin IVA (200 nM) (n = 7), calcium channel antagonists that potently block IPSPs in rat hippocampal neurons (Poncer et al., 2000). We considered the possibility that complete elimination of calcium influx prevents vesicular fusion more effectively than the other methods used above. However, the following experiments demonstrate that this was not the case, but indicate instead that calcium influx augments, but is not required for, GAT-1-mediated neurotransmission.

Recordings were made from pairs of cultured hippocampal neurons (naive to vigabatrin) in normal Ringer. After identifying synaptically coupled pairs in which the presynaptic neuron was GABAergic, the bath solution was changed to Ringer containing 0 mM Ca^{2+}, 1 mM EGTA, and Anemone Toxin II (ATx). ATx delays inactivation of sodium channels, and as described previously (Hartung and Rathmayer, 1985) this prolonged action potentials (Figure 7A). ATx also caused neurons to burst after they were stimulated by a train of depolarizing pulses (Figure 7B) and to occasionally burst spontaneously (Figure 7C, bottom trace). In one case, while recording in Ringer with 0 mM Ca^{2+}, 1 mM EGTA, and 5 nM ATx, we observed a large current in the postsynaptic neuron when the presynaptic GABAergic neuron spontaneously burst (Figure 7C). To determine whether this could be a nonvesicular GABAergic IPSC, we made paired recordings from synaptically coupled neurons in Ringer with 0 mM Ca^{2+}, 1 mM EGTA, and 5 nM ATx. Bursts of action potentials were induced in the presynaptic neuron by stimulation at 50 Hz for 9–20 s. This led to inward currents (Figure 7D) in 22 of 29 (76%) postsynaptic neurons (peak current 206 ± 26 pA). These calcium-independent IPSCs were due to GABA release, because they were blocked by gabazine (Figure 7D). The peak amplitude of IPSCs in gabazine was 7% ± 4% of that in zero calcium Ringer (p < 0.005; n = 8). The GABA release was due to GAT-1 reversal, because the IPSCs were also blocked by SKF-89976a (Figure 7E). The peak amplitude of IPSCs in

SKF-89976a was 9% ± 4% of that in zero calcium Ringer (p < 0.001; n = 11). It was not clear how much of the GABA release was due to action potentials versus tonic depolarization that sometimes followed the bursts. Either one alone could induce release since IPSCs could begin during bursts of action potentials (Figure 7C, vertical dashed lines), could occur when there were bursts without tonic depolarization (Figure 7B), or could be prolonged during the tonic depolarization phase (Figure 7C). Pressure microejection of 9 mM K$^+$ could also induce bursting in Ringer with 0 mM Ca^{2+}, 1 mM EGTA, and 5 nM ATx (data not shown). This was also associated with IPSCs that were blocked by SKF-89976a (Figure 7F).

The enhancement of nonvesicular GABA release by ATx described above is consistent with augmentation of Na$^+$ influx during prolonged action potentials, which would lead to a larger increase in cytosolic [Na$^+$] and a greater driving force for GAT-1 reversal.

Glutamate Transporters Do Not Reverse during High-Frequency Firing

It was not possible to elicit nonvesicular glutamatergic EPSCs. Patch-clamp recordings were made from 12 pairs of neurons in Ringer with 2 mM Ca^{2+}, 50 μM picrotoxin, and 1 μM CGP-55845 (GABA$_B$ antagonist). Postsynaptic responses obtained under these conditions were confirmed to be glutamatergic by blockade with CNQX (10 μM). When recordings were made from these neurons in high Mg^{2+}/low Ca^{2+} solution, it was not possible to elicit a response during high-frequency stimulation (50 Hz, 9 s), supporting the conclusion that high Mg^{2+}/low Ca^{2+} solution is effective in blocking vesicular fusion and also indicating that the glutamate transporter does not reverse under these conditions. These results are consistent with the fact that glutamate transporters have a different stoichiometry than GABA transporters and require a much higher membrane potential to reverse (Richerson and Wu, 2003; Wu et al., 2003; Zerangue and Kavanaugh, 1996). For this reason, it is predicted that glutamate transporters should only reverse under pathological conditions (Rossi et al., 2000).

DISCUSSION

The prevailing view of chemical synaptic transmission is that it occurs solely due to fusion of synaptic vesicles and that the only role of neurotransmitter transporters under physiological conditions is to recover released transmitter. Here we provide two lines of investigation that support the conclusion that GABA transporters play a more complex role.

Reversal Potential of GAT-1

The CHO cell assay we used to study GAT-1 reversal has several advantages. It is highly sensitive for detecting reversal of GABA transport, there is good control of membrane potential and substrate concentrations on the two sides of the membranes, and CHO cells do not have
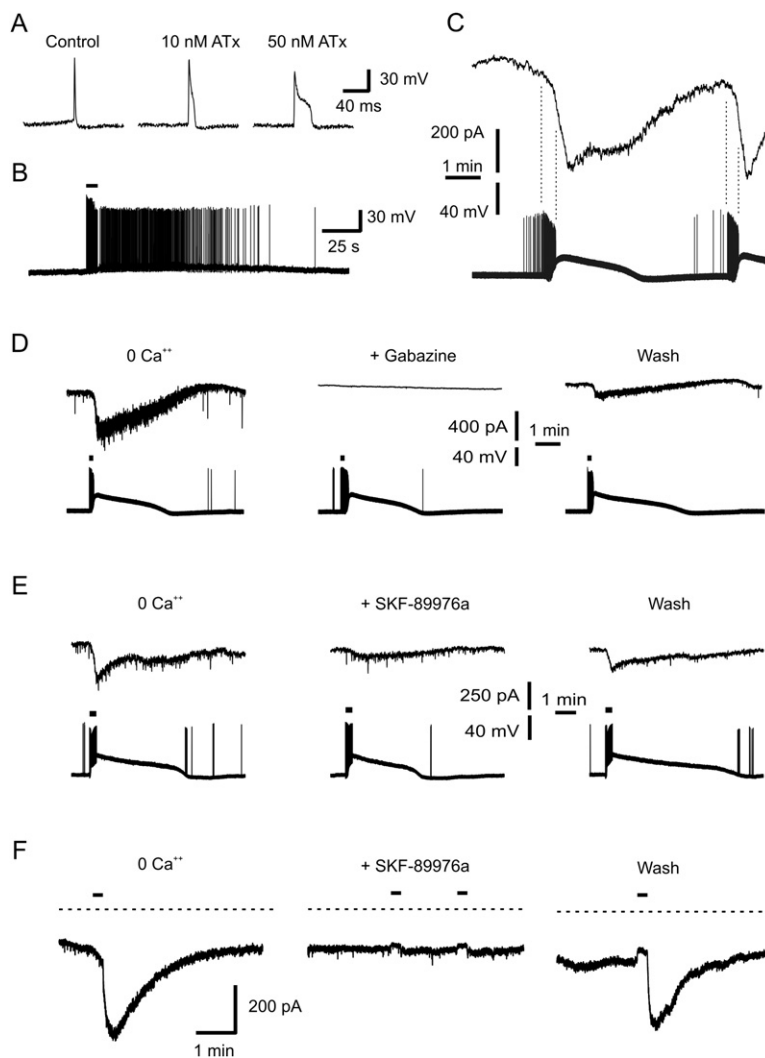
Figure 7. GABAergic Synaptic Transmission Could Be Induced in the Absence of Extracellular Ca^{2+} when Na^{+} Influx Was Enhanced by ATx

(A) ATx prolongs action potentials. Recordings were made in Ringer after treatment with 10 nM and 50 nM ATx.

(B) ATx caused some hippocampal neurons to burst in response to stimulation. This neuron was exposed to 10 nM Atx and stimulated with current injection (at bar).

(C) Simultaneous recording of two hippocampal neurons in Ringer with 0 mM Ca^{2+}, 1 mM EGTA, and 5 nM ATx. The neuron in the bottom trace (current clamp) was GABAergic and synapsed onto the neuron in the top trace (voltage clamp). ATx caused the GABAergic neuron to burst spontaneously, and this was associated with a large inward current in the postsynaptic neuron. Note that the inward current began during the burst (dashed lines) but continued during the tonic depolarization that followed.

(D) Simultaneous recording from two neurons in Ringer with 0 mM Ca^{2+}, 1 mM EGTA, and 5 nM ATx. Stimulation (50 Hz, 9 s, at bars) of the presynaptic GABAergic neuron (bottom traces) induced IPSCs in the postsynaptic neuron (top traces). The response was blocked by gabazine (40 μm).

(E) In another pair of neurons recorded under the same conditions, IPSCs were also blocked by SKF-89976a (40 μm).

(F) Under the same conditions as in (D), pressure microinjection of 9 mM K^{+} (at bars) led to a large inward current in this neuron. This stimulus also caused bursting of neurons (data not shown). The inward current was blocked by SKF-89976a (40 μm).

synaptic vesicles, so GAT-1-mediated GABA release can be studied in isolation. The results clearly demonstrate that when GABA translocation occurs it remains coupled to 2 Na^{+} and 1 Cl^{-} and support our previous prediction that under physiological conditions the reversal potential of GAT-1 is near the resting potential of neurons (Richerson and Wu, 2003). There were not many assumptions in making that prediction. The only parameters required for calculation of reversal potential are the intracellular and extracellular concentrations of Na^{+}, Cl^{-}, and GABA and the coupling ratio for GABA transport. Extracellular $[Na^{+}]$ and $[Cl^{-}]$ are known. Intracellular $[Na^{+}]$ has been measured to be 5–15 mM in neurons at rest (Rose, 2002). Intracellular $[Cl^{-}]$ is approximately 10 mM in many adult neurons, as assessed by measuring the reversal potential of $GABA_A$ receptor-mediated currents. The coupling ratio of 2 Na^{+}:1 Cl^{-}:1 GABA is widely accepted, and our experiments verify that this holds over a physiological range of substrate concentration. The only two parameters for which the values might be questioned are intracel-

lular and extracellular [GABA]. However, there are good reasons to believe the values we used were realistic.

Brain extracellular [GABA] has been reported to be 0.1–0.8 μM (Cavelier et al., 2005; Hagberg et al., 1985; Lerma et al., 1986; Phillis et al., 1994; Tossman et al., 1986). These measurements are likely to be accurate, because there is tonic inhibition of many neurons, and an ambient [GABA] this high would be needed to activate high-affinity $GABA_A$ receptors that have an EC_{50} of 0.2–0.4 μM (Saxena and Macdonald, 1996). Thus, our use of 0.1 μM for ambient [GABA] in our theoretical calculations and experimental protocol is reasonable.

A cytosolic [GABA] of 2 mM is also justified from the literature. It has been reported that cytosolic [GABA] ranges from 1 mM to 6 mM in mammalian neurons (Otsuka et al., 1971) and 10 mM in horizontal cells of fish retina (Schwartz, 1987). It is difficult to measure cytosolic [GABA] in neurons, so it is easy to be skeptical about these values. However, a value this high is consistent with results from magnetic resonance spectroscopy that have
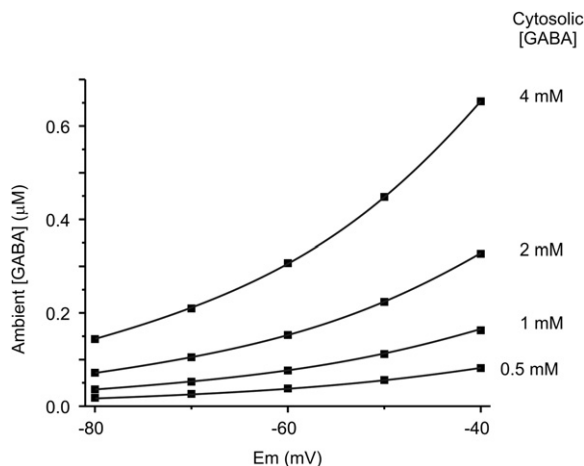
Figure 8. Theoretical Dependence of Ambient [GABA] on Membrane Potential and Cytosolic [GABA]

Shown are calculations of ambient [GABA] when GAT-1 is at equilibrium (i.e., driving force = 0). At a membrane potential of −60 mV, there will be no net transport of GABA when ambient [GABA] is between 0.04 μM and 0.3 μM for cytosolic [GABA] between 0.5 mM and 4 mM. These levels of ambient GABA span a range that would induce tonic inhibition of neurons expressing high-affinity GABA$_A$ receptors. Calculations were made assuming intracellular and extracellular [Na$^+$] and [Cl$^-$] of 150, 15, 135, and 10 mM, respectively.

measured average [GABA] in the human occipital lobe to be 1 mM (Rothman et al., 1993)—which would include a contribution from many nonGABAergic neurons and glia with a low [GABA]. Our use of 2 mM is also conservatively low given the conclusion of Hell and Jahn (1998) that cytosolic [GABA] is 5 mM or more since the Kd for the vesicular GABA transporter vGAT is 10 mM.

A cytosolic [GABA] of at least 2 mM in GABAergic neurons is also supported by the following logic. There is a significant amount of tonic inhibition in slices and in culture after vesicular GABA release is inhibited by zero calcium solution, tetanus toxin, and/or H$^+$-ATPase blockers (Hamann et al., 2002; Rossi et al., 2003; Wu et al., 2001, 2003, 2006). Under these conditions, it can be assumed that extracellular [GABA] is at least 0.1 μM, since [GABA] would need to be this high for tonic inhibition to occur. It can also be assumed that after blockade of synaptic GABA release GAT-1 would be able to reach its equilibrium, and thus the reversal potential for GAT-1 would be near the neuronal membrane potential. Therefore, the steady-state equation for the reversal potential of GAT-1 can be solved for cytosolic [GABA], since we have good estimates for all the other variables. If membrane potential = −60 mV, cytosolic [Na$^+$] = 10 mM, cytosolic [Cl$^-$] = 10 mM, ambient [Na$^+$] = 150 mM, ambient [Cl$^-$] = 135 mM, and ambient [GABA] = 0.1 μM, solving the equation (see below) at 37°C gives a cytosolic [GABA] of 2.9 mM. Although this is an estimate, it provides assurance that our use of 2 mM for cystosolic [GABA] is reasonable and that previous estimates and measurements of cytosolic [GABA] were relatively accurate. Intracellular

[Na$^+$] may be slightly higher in some neurons, and cytosolic [GABA] might be slightly lower, but over a fairly wide range the reversal potential would be relatively close to the normal resting potential of many neurons.

Role of GAT-1 in Regulating the Level of Tonic Inhibition

The data presented here have clear implications for regulation of tonic inhibition. It is widely believed that the major source of ambient GABA for tonic inhibition is spillover of synaptic GABA. This belief stems in part from the assumption that GABA transporters constantly operate in the forward direction at their maximum rate, and therefore any GABA that is present in the extracellular space must be there because it escaped the synaptic cleft before it could be scavenged by GAT-1. However, this is not a realistic view of transporter function. Instead, the rate of GABA reuptake is determined by the driving force on GABA transporters, and this driving force will become smaller as extracellular [GABA] decreases. Eventually the driving force becomes zero when ambient [GABA] decreases to the level at which GAT-1 is at equilibrium. We calculated the ambient [GABA] at which GAT-1 is at equilibrium for a neuron at four different levels of cytosolic GABA (Figure 8). The significance of these calculations is that GAT-1 would not be able to reduce ambient [GABA] below the values shown, even if there was no synaptic GABA release. If ambient [GABA] fell below these equilibrium values, GAT-1 would reverse to raise ambient [GABA] up to the equilibrium values. The surprising conclusion is that tonic inhibition does not exist simply because GABA transporters are unable to keep up with synaptic GABA release, leading to spillover, but instead because GAT-1 will not reduce ambient [GABA] below a level that is often high enough for tonic inhibition to occur. This can explain why the amount of tonic inhibition is relatively unaffected by inhibition of vesicular GABA release (Hamann et al., 2002; Rossi et al., 2003; Wu et al., 2006).

The anticonvulsants vigabatrin and gabapentin both increase brain GABA levels (Petroff et al., 1996; Rothman et al., 1993). This presumably includes an increase in neuronal cytosolic [GABA], which Figure 8 predicts would shift the setpoint for GAT-1 to a higher ambient [GABA]. This can explain why both drugs increase tonic inhibition (Cheng et al., 2006; Overstreet and Westbrook, 2001; Wu et al., 2001).

Reversal of GAT-1 during Action Potentials

Our data from CHO cells indicate that GAT-1 can reverse rapidly enough for GABA release to occur during action potentials. In fact, there are several reasons why reversal of GAT-1 might be less likely (or harder to detect) in our CHO cells compared to real neurons in vivo. First, our experiments were performed at room temperature, which reduces the rate of transport compared to body temperature (Gonzales et al., 2007). Second, the distance between GAT-1 cells and sniffer cells in our experiments was greater than the normal distance between neurons at

either synaptic or extrasynaptic regions, and the greater distance for diffusion would have slowed and attenuated the response. Third, in neurons the increase in intracellular $[Na^+]$ during a train of action potentials, which can reach 35 mM or higher (Rose, 2002; Rose and Ransom, 1997), would enhance GAT-1 reversal (Figure 2C), and this would not occur in CHO cells since they do not express voltage-dependent sodium channels. Therefore, the data from CHO cells suggest that it would be surprising if GAT-1 did not reverse in neurons in response to high-frequency firing.

Our data from hippocampal neurons demonstrate that GAT-1 does reverse during high-frequency firing. These data include the following. (1) IPSCs were not blocked by tetanus toxin, concanamycin A, or high Mg^{2+}/low Ca^{2+} solution alone or in combination. (2) IPSCs occurred in the absence of extracellular calcium when Na^+ influx was enhanced by ATx. (3) IPSCs under each of these conditions were completely blocked by highly specific GAT-1 antagonists at low concentrations. (4) Nonvesicular IPSCs were enhanced by vigabatrin, which increases nonvesicular GABA release but decreases vesicular neurotransmission (Overstreet and Westbrook, 2001; Wu et al., 2003). (5) Similar results were not obtained at glutamatergic synapses, consistent with a higher theoretical reversal potential for glutamate transporters.

Our results indicate that extracellular calcium influences GAT-1-mediated GABA release. This was not due to a direct effect, since GAT-1 was unaffected by calcium in our CHO cell assay. We propose the following model to explain the effect of calcium. During an action potential, GAT-1 reversal occurs due to both depolarization and a rise in $[Na^+]$ within presynaptic terminals. The increase in cytosolic $[Na^+]$ is due to (1) influx of Na^+ via voltage-dependent Na^+ channels and (2) influx of Na^+ via the Na/Ca exchanger in the process of extrusion of Ca^{2+} that has entered the terminal via voltage-dependent Ca^{2+} channels. This is consistent with previous work showing that Na/Ca exchange makes a major contribution to the rise of intracellular $[Na^+]$ during activity (Regehr, 1997). Our data demonstrate that lowering extracellular Ca^{2+} reduces GAT-1-mediated GABA release, but this can be overcome simply by enhancing Na^+ influx via Na^+ channels. Thus, nonvesicular IPSCs are sensitive to extracellular Ca^{2+}, but are not dependent on it.

The fact that GABAergic neurotransmission can occur due to reversal of the GABA transporter may seem surprising, but there is abundant evidence that depolarization induces transporter-mediated GABA release (Belhage et al., 1993; Cammack et al., 1994; Gaspary et al., 1998; Pin and Bockaert, 1989; Richerson and Wu, 2003; Schwartz, 1982, 1987; Wu et al., 2001, 2003). There is experimental and theoretical evidence that this transporter reversal can occur under physiological conditions (Bernath and Zigmond, 1988; Richerson and Wu, 2003; Wu et al., 2003). Our results should also not be surprising given the direct demonstration that GABA transporter reversal can mediate GABAergic neurotransmission be-

tween fish retinal neurons (Schwartz, 1987), and evidence that a similar phenomenon occurs in the rabbit retina (O'Malley et al., 1992). Reversal of the dopamine transporter, which has a similar stoichiometry, has also been shown to support communication between neurons in the substantia nigra (Falkenburger et al., 2001). Thus, the phenomenon we demonstrate here is expected from a theoretical viewpoint, in context with the existing literature and in light of our new data from CHO cells.

GABA transporters are widely believed to operate slowly (Mager et al., 1993). However, recent data indicate that the turnover rate for GAT-1 is faster than previously believed, taking 66 ms per translocation cycle at 21°C and 11 ms per translocation cycle at 37°C (Gonzales et al., 2007). However, this would still be too long for a complete cycle to occur during an action potential that lasts only a few milliseconds. Therefore, depolarization may lead to GABA release from GAT-1 molecules that have already undergone voltage-independent transitions between states prior to depolarization. Alternatively, it is not known how long it takes to complete each step in a translocation cycle, and it is possible that GAT-1 may release GABA rapidly in response to depolarization by completing only a subset of steps in a cycle. In the future it will be important to directly address questions such as this about the molecular dynamics of the release process.

Relevance to Neurotransmission In Vivo
Our results from neurons were obtained in cell culture, and it is not clear whether GABA transporter reversal would also occur in vivo. If GAT-1 reversal does not occur normally, it is possible that it is enhanced under some conditions in vivo. For example, during seizures, depolarization and increased intracellular $[Na^+]$ during bursts would both enhance GAT-1 reversal, consistent with direct measurements of GABA release in the human temporal lobe using microdialysis (During et al., 1995). In dentate granule cells, kainic acid-induced seizures lead to an increase in expression of glutamic acid decarboxylase and GAT-1 (Sperk et al., 2003), which would both also enhance GAT-1-mediated GABA release.

Our results may overestimate the contribution of nonvesicular release, because vesicular release was blocked in our experimental paradigm, and GAT-1-mediated GABA release is not independent of vesicular GABA release. When vesicular release occurs, it would be less likely that GAT-1 would reverse, because the increase in extracellular [GABA] due to vesicular release would increase the inward gradient for GABA transport, as predicted by theoretical calculations (Richerson and Wu, 2003). In this case, our results can be interpreted as indicating that there would be a reduction in the driving force for GABA uptake during neuronal firing, rather than frank reversal. This could explain why blocking GABA transporters does not always lead to an increase in amplitude or duration of IPSPs (Dingledine and Korn, 1985; Isaacson et al., 1993; Nusser and Mody, 2002).

Our results also do not address related questions about the behavior of GAT-1 at synaptic versus extrasynaptic sites. Synaptic and perisynaptic GAT-1 may not reverse as easily in vivo due to coexisting vesicular GABA release. However, our results may be particularly relevant to the behavior of extrasynaptic GAT-1. As neuronal firing increases there would be an increase in the extrasynaptic [GABA] at which GAT-1 is at equilibrium, which would be predicted to increase tonic inhibition.

Conclusions

The results described here indicate that GAT-1, in addition to recovering extracellular GABA after vesicular release, plays an important role in regulating the level of tonic inhibition by attempting to clamp ambient [GABA] at a relatively high level. Our findings also indicate that GAT-1 is highly dynamic, being capable of changing direction rapidly and frequently. Nonvesicular GABAergic neurotransmission may be a primitive form of synaptic communication that is complementary to vesicular fusion and has been retained as a fail-safe release mechanism in the mammalian CNS. This feature of the GABAergic system, which is not shared by the glutamatergic system, may play a critical role in maintaining inhibition during high-frequency firing when vesicular fusion begins to fail, acting as a brake to prevent runaway excitation. Nonvesicular GABA release, which is increased by two novel anticonvulsants, gabapentin (Cheng et al., 2006; Honmou et al., 1995) and vigabatrin (Wu et al., 2001, 2003), may play a critical role in control of brain excitability and may be a new target for physiological and pharmacological modulation (Deken et al., 2001; Whitworth and Quick, 2001).

EXPERIMENTAL PROCEDURES

CHO Cell Transfection

Chinese hamster ovary cells (CHO cells) were grown in Iscoves's modified Dulbecco's medium supplemented with 10% fetal bovine serum, sodium hypoxanthine, thymidine, and penicillin/streptomycin (all from Invitrogen). Cells were split when they were confluent and plated on glass coverslips in 12-well Falcon plates 1 or 2 days before transfection. Transfection was performed using lipofectamine (4 μl/well; Life Technologies).

Rat GAT-1 (*Slc6a1*) cDNA was subcloned into a pIRES2-EGFP vector (Clontech) and transfected using 1.6 μg of DNA per well. Rat GABA$_A$ receptor α6 subunit (*Gabra6*) cDNA was subcloned into a pIRES2-EGFP vector. Rat β3 (*Gabrb3*) and δ (*Gabrd*) subunit cDNAs were subcloned in a pCMV vector. For transfection of GABA receptors, a total of 2.87 μg of DNA was used per well, in a ratio of 1 α6:2 β3:2 δ. This ratio was used to increase the chance that every green cell (those expressing the α6 subunit) also expressed β3 and δ subunits.

Cell Culture

Primary cell cultures of hippocampal neurons and glia were prepared from neonatal (P0-P2) Sprague-Dawley rats as described previously (Gaspary et al., 1998; Wu et al., 2001, 2003). Culture wells were supplemented with culture medium to which vigabatrin, tetanus toxin, or concanamycin A were added in the appropriate concentration (using a 10–100× stock), and then maintained in an incubator until recording. All culture experiments were performed on neurons pretreated with 100 μM vigabatrin (usually for 3–5 days), with three exceptions: (1)

comparing IPSCs with and without vigabatrin treatment; (2) measuring the effect of ATx on IPSCs in zero calcium solution; and (3) testing for nonvesicular glutamatergic EPSCs.

Electrophysiology
CHO Cells

One day after transfection, two coverslips were placed in a recording chamber mounted on the stage of an inverted light microscope (Axiovert 100, Zeiss), one with CHO cells transfected with GAT-1 and the other with CHO cells transfected with GABA$_A$ receptors. The recording chamber was irrigated at 2–3 ml/min with Ringer (in mM): NaCl 124, KCl 3, CaCl$_2$ 2, MgCl$_2$ 2, NaHCO$_3$ 26, NaH$_2$PO$_4$ 1.3, dextrose 10; pH 7.4 after bubbling with 95% O$_2$/5% CO$_2$. Transfected cells were identified by visualizing GFP fluorescence. The bath solution for individual experiments was modified from that described above, as indicated in the text. All experiments were performed at room temperature.

Patch-clamp recording electrodes (1.4–3.0 MΩ) were fabricated from thin-walled, borosilicate glass tubing with a micropipette puller (Sutter Instruments, Model P-87, Novato, CA). Whole-cell patch-clamp recordings were made from GAT-1 cells with an electrode solution that contained various concentrations of Na$^+$, Cl$^-$, and GABA as indicated. For example, the control solution with 15 mM Na$^+$, 10 mM Cl$^-$, and 2 mM GABA contained (in mM) NaCl 10, NaOH 5, KOH 115, methanesulfonic acid 120, GABA 2, N-[2-hydroxyethyl]piperazine-N′-[2-ethanesulfonic acid] (HEPES) 10, ethylene glycol-bis (β-aminoethyl ether)-N,N,N′,N′-tetraacetic acid (EGTA) 1, (pH adjusted to 7.2 with KOH). Changes in [Na$^+$] were made by adjusting the concentrations of NaCl, NaOH, KOH, and/or KCl to maintain constant [Cl$^-$] and osmolarity. Changes in [Cl$^-$] were made by adjusting the concentrations of NaCl, NaOH, KOH, KCl, and/or methanesulfonic acid to maintain constant [Na$^+$], [K$^+$], and osmolarity. When changes in [GABA] were made, the concentrations of KOH and methanesulfonic acid were adjusted to maintain constant osmolarity. The GAT-1 cell was lifted off its coverslip and moved over to the other coverslip to touch a CHO cell transfected with GABA$_A$ receptors. A second whole-cell patch-clamp recording was made from the sniffer cell with an electrode solution that contained (in mM) KCl 135, HEPES 10, EGTA 1 (KOH to pH 7.2). This resulted in a Nernst potential for Cl$^-$ of 0 mV.

Patch-clamp recordings were made using a MultiClamp 700A amplifier (Axon Instruments, Foster City, CA). Recordings were filtered, digitized, and stored on computer using a commercially available data acquisition system (Digidata 1322A and PClamp software, Axon Instruments). Recordings from both CHO cells were made in voltage-clamp mode at a holding potential of −60 mV. Voltage steps and voltage ramps (as described) were induced in the GAT-1 cell to determine the voltage dependence of GAT-1-mediated GABA release. For the experiments shown in Figure 3C, the voltage-clamp command supplied to the patch-clamp amplifier was derived from a data file obtained from a current-clamp recording of action potentials in a cultured neuron. Steady-state currents induced in sniffer cells were quantified using Clampfit software (Axon Instruments).

Paired Hippocampal Neurons

For recordings from neurons, coverslips were placed in a chamber on a fixed stage upright light microscope (Axioskop FS, Carl Zeiss) and superfused (at 3–4 ml/min) with one of the following solutions. Ringer contained (in mM) NaCl 124, KCl 3, MgCl$_2$ 2, CaCl$_2$ 2, NaH$_2$PO$_4$ 1.3, NaHCO$_3$ 26, dextrose 10, the GABA$_B$ receptor antagonist CGP-55845 (1 μM), and the glutamate receptor antagonists 6-cyano-7-nitroquinoxaline-2,3-dione (CNQX; 10 μM), and (±)-2-amino-5-phosphonopentanoic acid (AP-5; 50 μM). High Mg^{2+}/low Ca^{2+} Ringer was the same solution (including receptor antagonists) except CaCl$_2$ was reduced to 0.2 mM, MgCl$_2$ was increased to 10 mM, NaCl was reduced to 117 mM, and KCl was reduced to 1 mM. Zero calcium solution was the same as Ringer, except that CaCl$_2$ was omitted and 1 mM EGTA was added. For some experiments with zero calcium solution, kynurenic acid (1 mM) was substituted for CNQX and AP-5. Bath solutions were bubbled with 5% CO$_2$/95% O$_2$ at pH 7.4. For a small number

of experiments (Figure 7F), a pressure microejection system was used to apply zero calcium Ringer modified to increase KCl to 9 mM and decrease NaCl to 118 mM. All experiments were performed at room temperature.

Whole-cell patch-clamp recordings were made from two neurons using either two Axopatch 1D amplifiers or a MultiClamp 700A amplifier (Axon Instruments). Recordings were first made in normal Ringer to identify neuron pairs in which stimulation of one induced a GABAergic IPSC in the other. The bath solution was then switched to one of the other solutions described above. Identification of presynaptic GABAergic neurons was initially performed by trial and error. Later, the yield of useful recordings was increased by choosing neurons based on morphology. The postsynaptic neuron was recorded in voltage-clamp mode at a holding potential of −50 mV. The presynaptic neuron was recorded in current-clamp mode and stimulated (50 Hz, 9–20 s) with sufficient current to insure that each stimulus induced an action potential. Recordings were filtered, digitized, and stored on computer using a commercially available data acquisition system (TL-1 DMA or Digidata 1322A, and PClamp software, Axon Instruments). Recording electrodes (2.5–4.0 MΩ) were fabricated from thin-walled, borosilicate glass tubing (Diamond General, Ann Arbor, MI). For most experiments, patch-clamp electrodes were filled with solution containing (in mM) methanesulfonic acid 135, KOH 130, KCl 2, HEPES 5, EGTA 1, NaOH 5, and GABA 5. In a small number of recordings, NaOH and GABA were decreased to 0 mM each or increased to 20 mM each (KOH and methanesulfonic acid were adjusted to maintain osmolarity). These recordings gave the same general results and contributed to the "n" values, but these data were not included in the quantitative analyses. For the zero calcium experiments presented in Figure 7, the presynaptic electrode contained (in mM) NaCl 10, NaOH 5, KOH 115, methanesulfonic acid 120, HEPES 10, EGTA 1, and GABA 5. The postsynaptic electrode contained (in mM) QX-314 10, CsCl 124, HEPES 10, and EGTA 10. This solution caused $GABA_A$ receptor-mediated currents to be inward instead of outward. Electrode solutions were adjusted to pH 7.2 with KOH or CsOH and to an osmolarity of 270 ± 5 mOsm with dH_2O. Initial seal resistance was ≥1 GΩ. Whole-cell access was typically 10–20 MΩ. Although we used whole-cell recordings and this could potentially influence the driving force for GAT-1 reversal, we found that the composition of the solution in the whole-cell recording pipette used for the presynaptic neuron had no effect on IPSCs, even when [Na⁺] and [GABA] were elevated to high levels. This was probably because GABA and Na⁺ within the soma were not able to diffuse to distant presynaptic terminals.

Data Analysis
Measurement of Reversal Potential Using Ramp Protocols
To measure the reversal potential of GAT-1, we used voltage-clamp recordings from sniffer cells to measure the current induced in response to ramp depolarization of a GAT-1 cell as shown in Figure 2A. An individual blind to the calculation of the reversal potential drew a horizontal line through the flat portion of the moving average. A vertical line was then drawn at the first point at which the moving average dropped below the horizontal line and did not return (i.e., when GABA release first began to occur). There was some drift in the baseline in some cases, but the point at which there was divergence from the baseline could be reliably identified with consistent values obtained on repeat analysis. The voltage at which this vertical line intersected the voltage-clamp command trace was defined as the reversal potential for GAT-1.
Analysis of IPSCs
Data analysis was performed using either custom-written analysis routines (OriginLab Corp, Northampton, MA) or a commercially available analysis program (Clampfit, Axon Instruments), in both cases using signal-averaging techniques. IPSCs in high Mg^{2+}/low Ca^{2+} Ringer were quantified as the integral of the baseline-subtracted current in picocoulombs. IPSCs in normal Ringer and zero calcium Ringer were quantified as the peak amplitude (difference between the peak

current and the prestimulus baseline current) in picoamps. Steady-state amplitude was determined as the mean amplitude for the last 2 s of an IPSC.

All values expressed as x ± y are mean ± SEM, and all error bars are SEM.

Thermodynamic Equations Describing GAT-1
As previously described (Richerson and Wu, 2003), the equation used to calculate the reversal potential for GAT-1 was derived by rearranging the equation for the electrochemical driving force for GAT-1 when it is at equilibrium (i.e., driving force = 0). This equation is expressed as

$$E_m = \frac{R \cdot T}{(2 \cdot Z_{Na} + Z_{Cl})F} \cdot \ln\left[\frac{[GABA]_{out}}{[GABA]_{in}} \cdot \left(\frac{[Na^+]_{out}}{[Na^+]_{in}}\right)^2 \cdot \frac{[Cl^-]_{out}}{[Cl^-]_{in}}\right]$$

where E_m = reversal potential, Z_x = the valence of ion X, F = Faraday's constant, R = universal gas constant, and T = temperature (295°K). There is a useful website that calculates the solution to this equation for any combination of variables at http://www.csupomona.edu/~seskandari/physiology/physiological_calculators/gat_v_rev.html. To calculate ambient [GABA] when GAT-1 is at equilibrium (Figure 8), we rearranged the above equation to solve for [GABA]_{out} with membrane potential as a variable.

REFERENCES
Albus, U., and Habermann, E. (1983). Tetanus toxin inhibits the evoked outflow of an inhibitory (GABA) and an excitatory (D-aspartate) amino acid from particulate brain cortex. Toxicon 21, 97–110.

Aronson, P.S., Boron, W.F., and Boulpaep, E.L. (2003). Physiology of membranes. In Medical Physiology: A Cellular and Molecular Approach, W.F. Boron and E.L. Boulpaep, eds. (Philadelphia, PA: Saunders), pp. 50–86.

Attwell, D., Barbour, B., and Szatkowski, M. (1993). Nonvesicular release of neurotransmitter. Neuron 11, 401–407.

Belhage, B., Hansen, G.H., and Schousboe, A. (1993). Depolarization by K⁺ and glutamate activates different neurotransmitter release mechanisms in GABAergic neurons: vesicular versus non-vesicular release of GABA. Neuroscience 54, 1019–1034.

Bernath, S., and Zigmond, M.J. (1988). Characterization of [³H]GABA release from striatal slices: evidence for a calcium-independent process via the GABA uptake system. Neuroscience 27, 563–570.

Bianchi, M.T., Haas, K.F., and Macdonald, R.L. (2002). α1 and α6 subunits specify distinct desensitization, deactivation and neurosteroid modulation of $GABA_A$ receptors containing the δ subunit. Neuropharmacology 43, 492–502.

Borden, L.A. (1996). GABA transporter heterogeneity: pharmacology and cellular localization. Neurochem. Int. *29*, 335–356.

Brickley, S.G., Revilla, V., Cull-Candy, S.G., Wisden, W., and Farrant, M. (2001). Adaptive regulation of neuronal excitability by a voltage-independent potassium conductance. Nature *409*, 88–92.

Cammack, J.N., Rakhilin, S.V., and Schwartz, E.A. (1994). A GABA transporter operates asymmetrically and with variable stoichiometry. Neuron *13*, 949–960.

Cavelier, P., Hamann, M., Rossi, D., Mobbs, P., and Attwell, D. (2005). Tonic excitation and inhibition of neurons: ambient transmitter sources and computational consequences. Prog. Biophys. Mol. Biol. *87*, 3–16.

Cheng, V.Y., Bonin, R.P., Chiu, M.W., Newell, J.G., MacDonald, J.F., and Orser, B.A. (2006). Gabapentin increases a tonic inhibitory conductance in hippocampal pyramidal neurons. Anesthesiology *105*, 325–333.

Deken, S.L., Beckman, M.L., and Quick, M.W. (2001). PICKing on transporters. Trends Neurosci. *24*, 623–625.

Dingledine, R., and Korn, S.J. (1985). Gamma-aminobutyric acid uptake and the termination of inhibitory synaptic potentials in the rat hippocampal slice. J. Physiol. *366*, 387–409.

During, M.J., Ryder, K.M., and Spencer, D.D. (1995). Hippocampal GABA transporter function in temporal-lobe epilepsy. Nature *376*, 174–177.

Falkenburger, B.H., Barstow, K.L., and Mintz, I.M. (2001). Dendrodendritic inhibition through reversal of dopamine transport. Science *293*, 2465–2470.

Gaspary, H.L., Wang, W., and Richerson, G.B. (1998). Carrier-mediated GABA release activates GABA receptors on hippocampal neurons. J. Neurophysiol. *80*, 270–281.

Gonzales, A.L., Lee, W., Spencer, S., Oropeza, R.A., Chapman, J., Ku, J., and Eskandari, S. (2007). Turnover rate of the γ-aminobutyric acid transporter GAT1. J. Membr. Biol., in press. Published online November 10, 2007. 10.1007/s00232.007.9073.5.

Hagberg, H., Lehmann, A., Sandberg, M., Nystrom, B., Jacobson, I., and Hamberger, A. (1985). Ischemia-induced shift of inhibitory and excitatory amino acids from intra- to extracellular compartments. J. Cereb. Blood Flow Metab. *5*, 413–419.

Hamann, M., Rossi, D.J., and Attwell, D. (2002). Tonic and spillover inhibition of granule cells control information flow through cerebellar cortex. Neuron *33*, 625–633.

Hartung, K., and Rathmayer, W. (1985). Anemonia sulcata toxins modify activation and inactivation of Na$^+$ currents in a crayfish neurone. Pflugers Arch. *404*, 119–125.

Hell, J.W., and Jahn, R. (1998). Bioenergetic characterization of gamma-aminobutyric acid transporter of synaptic vesicles. Methods Enzymol. *296*, 116–124.

Honmou, O., Kocsis, J.D., and Richerson, G.B. (1995). Gabapentin potentiates the conductance increase induced by nipecotic acid in CA1 pyramidal neurons in vitro. Epilepsy Res. *20*, 193–202.

Isaacson, J.S., Solis, J.M., and Nicoll, R.A. (1993). Local and diffuse synaptic actions of GABA in the hippocampus. Neuron *10*, 165–175.

Kahlig, K.M., Binda, F., Khoshbouei, H., Blakely, R.D., McMahon, D.G., Javitch, J.A., and Galli, A. (2005). Amphetamine induces dopamine efflux through a dopamine transporter channel. Proc. Natl. Acad. Sci. USA *102*, 3495–3500.

Kanner, B.I., and Schuldiner, S. (1987). Mechanism of transport and storage of neurotransmitters. CRC Crit. Rev. Biochem. *22*, 1–38.

Krause, S., and Schwarz, W. (2005). Identification and selective inhibition of the channel mode of the neuronal GABA transporter 1. Mol. Pharmacol. *68*, 1728–1735.

Lerma, J., Herranz, A.S., Herreras, O., Abraira, V., and del Rio, M. (1986). In vivo determination of extracellular concentration of amino acids in the rat hippocampus. A method based on brain dialysis and computerized analysis. Brain Res. *384*, 145–155.

Levi, G., and Raiteri, M. (1993). Carrier-mediated release of neurotransmitters. Trends Neurosci. *16*, 415–419.

Lu, C.C., and Hilgemann, D.W. (1999). GAT1 (GABA:Na$^+$:Cl$^-$) cotransport function. Steady state studies in giant *Xenopus* oocyte membrane patches. J. Gen. Physiol. *114*, 429–444.

Mager, S., Naeve, J., Quick, M., Labarca, C., Davidson, N., and Lester, H.A. (1993). Steady states, charge movements, and rates for a cloned GABA transporter expressed in Xenopus oocytes. Neuron *10*, 177–188.

Nusser, Z., and Mody, I. (2002). Selective modulation of tonic and phasic inhibitions in dentate gyrus granule cells. J. Neurophysiol. *87*, 2624–2628.

O'Malley, D.M., Sandell, J.H., and Masland, R.H. (1992). Co-release of acetylcholine and GABA by the starburst amacrine cells. J. Neurosci. *12*, 1394–1408.

Otsuka, M., Obata, K., Miyata, Y., and Tanaka, Y. (1971). Measurement of γ-aminobutyric acid in isolated nerve cells of cat central nervous system. J. Neurochem. *18*, 287–295.

Overstreet, L.S., and Westbrook, G.L. (2001). Paradoxical reduction of synaptic inhibition by vigabatrin. J. Neurophysiol. *86*, 596–603.

Overstreet, L.S., and Westbrook, G.L. (2003). Synapse density regulates independence at unitary inhibitory synapses. J. Neurosci. *23*, 2618–2626.

Pearce, B.R., Gard, A.L., and Dutton, G.R. (1983). Tetanus toxin inhibition of K$^+$-stimulated [^{3}H]GABA release from developing cell cultures of the rat cerebellum. J. Neurochem. *40*, 887–890.

Petroff, O.A., Rothman, D.L., Behar, K.L., Lamoureux, D., and Mattson, R.H. (1996). The effect of gabapentin on brain γ-aminobutyric acid in patients with epilepsy. Ann. Neurol. *39*, 95–99.

Phillis, J.W., Smith-Barbour, M., Perkins, L.M., and O'Regan, M.H. (1994). Characterization of glutamate, aspartate, and GABA release from ischemic rat cerebral cortex. Brain Res. Bull. *34*, 457–466.

Pin, J.P., and Bockaert, J. (1989). Two distinct mechanisms, differentially affected by excitatory amino acids, trigger GABA release from fetal mouse striatal neurons in primary culture. J. Neurosci. *9*, 648–656.

Poncer, J.C., McKinney, R.A., Gahwiler, B.H., and Thompson, S.M. (2000). Differential control of GABA release at synapses from distinct interneurons in rat hippocampus. J. Physiol. *528*, 123–130.

Regehr, W.G. (1997). Interplay between sodium and calcium dynamics in granule cell presynaptic terminals. Biophys. J. *73*, 2476–2488.

Richerson, G.B., and Wu, Y. (2003). The dynamic equilibrium of neurotransmitter transporters: Not just for reuptake anymore. J. Neurophysiol. *90*, 1363–1374.

Roepstorff, A., and Lambert, J.D. (1992). Comparison of the effect of the GABA uptake blockers, tiagabine and nipecotic acid, on inhibitory synaptic efficacy in hippocampal CA1 neurones. Neurosci. Lett. *146*, 131–134.

Rose, C.R. (2002). Na$^+$ signals at central synapses. Neuroscientist *8*, 532–539.

Rose, C.R., and Ransom, B.R. (1997). Regulation of intracellular sodium in cultured rat hippocampal neurones. J. Physiol. *499*, 573–587.

Rossi, D.J., Oshima, T., and Attwell, D. (2000). Glutamate release in severe brain ischaemia is mainly by reversed uptake. Nature *403*, 316–321.

Rossi, D.J., Hamann, M., and Attwell, D. (2003). Multiple modes of GABAergic inhibition of rat cerebellar granule cells. J. Physiol. *548*, 97–110.

Rothman, D.L., Petroff, O.A., Behar, K.L., and Mattson, R.H. (1993). Localized ^{1}H NMR measurements of γ-aminobutyric acid in human brain in vivo. Proc. Natl. Acad. Sci. USA *90*, 5662–5666.

Saxena, N.C., and Macdonald, R.L. (1996). Properties of putative cerebellar γ-aminobutyric acid$_A$ receptor isoforms. Mol. Pharmacol. *49*, 567–579.

Schwartz, E.A. (1982). Calcium-independent release of GABA from isolated horizontal cells of the toad retina. J. Physiol. *323*, 211–227.

Schwartz, E.A. (1987). Depolarization without calcium can release γ-aminobutyric acid from a retinal neuron. Science *238*, 350–355.

Sperk, G., Schwarzer, C., Heilman, J., Furtinger, S., Reimer, R.J., Edwards, R.H., and Nelson, N. (2003). Expression of plasma membrane GABA transporters but not of the vesicular GABA transporter in dentate granule cells after kainic acid seizures. Hippocampus *13*, 806–815.

Sudhof, T.C. (2001). α-Latrotoxin and its receptors: Neurexins and CIRL/latrophilins. Annu. Rev. Neurosci. *24*, 933–962.

Thompson, S.M., and Gahwiler, B.H. (1992). Effects of the GABA uptake inhibitor tiagabine on inhibitory synaptic potentials in rat hippocampal slice cultures. J. Neurophysiol. *67*, 1698–1701.

Tossman, U., Jonsson, G., and Ungerstedt, U. (1986). Regional distribution and extracellular levels of amino acids in rat central nervous system. Acta Physiol. Scand. *127*, 533–545.

Turner, T.J., and Goldin, S.M. (1989). Multiple components of synaptosomal [^{3}H]-gamma-aminobutyric acid release resolved by a rapid superfusion system. Biochemistry *28*, 586–593.

Whitworth, T.L., and Quick, M.W. (2001). Upregulation of gamma-aminobutyric acid transporter expression: role of alkylated gamma-aminobutyric acid derivatives. Biochem. Soc. Trans. *29*, 736–741.

Wu, Y., Wang, W., and Richerson, G.B. (2001). GABA transaminase inhibition induces spontaneous and enhances depolarization-evoked GABA efflux via reversal of the GABA transporter. J. Neurosci. *21*, 2630–2639.

Wu, Y., Wang, W., and Richerson, G.B. (2003). Vigabatrin induces tonic inhibition via GABA transporter reversal without increasing vesicular GABA release. J. Neurophysiol. *89*, 2021–2034.

Wu, Y., Wang, W., and Richerson, G.B. (2006). The transmembrane sodium gradient influences ambient GABA concentration by altering the equilibrium of GABA transporters. J. Neurophysiol. *96*, 2425–2436.

Yunger, L.M., Fowler, P.J., Zarevics, P., and Setler, P.E. (1984). Novel inhibitors of γ-aminobutyric acid (GABA) uptake: anticonvulsant actions in rats and mice. J. Pharmacol. Exp. Ther. *228*, 109–115.

Zerangue, N., and Kavanaugh, M.P. (1996). Flux coupling in a neuronal glutamate transporter. Nature *383*, 634–637.

Zhu, L., Lovinger, D., and Delpire, E. (2005). Cortical neurons lacking KCC2 expression show impaired regulation of intracellular chloride. J. Neurophysiol. *93*, 1557–1568.